Dittrich, M., Mueller, H. M., Bauer, H., Peirats-Llobet, M., Rodriguez, P. L., Geilfus, C.-M., Carpentier, S. C., Al-Rasheid, K. A. S., Kollist, H., Merilo, E., Herrmann, J., Müller, T., Ache, P., Hetherington, A. M., & Hedrich, R. (2019). The role of Arabidopsis ABA receptors from the PYR/PYL/RCAR family in stomatal acclimation and closure signal integration. *Nature Plants*, *5*, 1002-1011. https://doi.org/10.1038/s41477-019-0490-0

Peer reviewed version

Link to published version (if available):
10.1038/s41477-019-0490-0

Link to publication record on the Bristol Research Portal
PDF-document

The role of Arabidopsis ABA receptors from the PYR/PYL/RCAR family in stomatal acclimation and closure signal integration.

Marcus Dittrich[1,2†], Heike M. Mueller[3†], Hubert Bauer[3], Marta Peirats-Llobet[4], Pedro L. Rodriguez[4], Christoph-Martin Geilfus[5], Sebastien Christian Carpentier[6,7], Khaled A. S. Al Rasheid[8]; Hannes Kollist[9]; Johannes Herrmann[3], Tobias Müller[1*], Peter Ache[3], Alistair M. Hetherington[10*], and Rainer Hedrich[3]

[1] Department of Bioinformatics, University of Würzburg, D-97074 Würzburg, Germany;

[2] Department of Human Genetics, University of Würzburg, D-97074 Würzburg, Germany;

[3] Institute for Molecular Plant Physiology and Biophysics, Biocenter, University Wuerzburg, D-97082 Wuerzburg, Germany;

[4] Instituto de Biología Molecular y Celular de Plantas, Consejo Superior de Investigaciones Cientificas-Universidad Politecnica de Valencia, ES-46022 Valencia, Spain;

[5] Division of Controlled Environment Horticulture, Faculty of Life Sciences, Albrecht Daniel Thaer-Institute of Agricultural and Horticultural Sciences, Humboldt-University of Berlin, Albrecht-Thaer-Weg 1, 14195 Berlin, Germany;

[6] SYBIOMA, Proteomics Core Facility, KU Leuven, O&N II Herestraat 49 - bus 901, B-3000 Leuven, Belgium;

[7] Division of Crop Biotechnics, Department of Biosystems, KU Leuven, Willem de Croylaan 42 - box 2455, B-3001 Leuven, Belgium;

[8] Zoology Department, College of Science, King Saud University, Riyadh 11451, Saudi Arabia;

[9] Institute of Technology, University of Tartu, Tartu, Estonia;

[10] School of Biological Sciences, University of Bristol, Bristol BS8 1TQ, United Kingdom

[*] Correspondence: Tobias.Mueller@biozentrum.uni-wuerzburg.de and Alistair.Hetherington@bristol.ac.uk

[†] M.D. and H.M.M. contributed equally to this work

Abstract

Stomata are microscopic pores found on the surfaces of leaves which act to control CO_2 uptake and water loss. By integrating information derived from endogenous signals with cues from the surrounding environment the guard cells, that surround the pore, 'set' stomatal aperture to suit the prevailing conditions. Much research has concentrated on understanding the rapid intracellular changes that result in immediate changes to stomatal aperture. In this study we look instead at how stomata acclimate to longer timescale variations in their environment. We show that the closure-inducing signals ABA, increased CO_2, decreased relative air humidity (RH), and darkness each access a unique gene network made up of clusters (or modules) of common cellular processes. However, within these some gene clusters are shared among all four stimuli. All stimuli modulate the expression of members of the PYR/PYL/RCAR family of ABA receptors, however these are modulated differentially in a stimulus-specific manner. Of the six members of the PYR/PYL/RCAR family expressed in guard cells, PYL2 is sufficient for guard cell ABA-induced responses. Whereas, in the responses to CO_2 PYL4 and PYL5 are

essential. Overall our work shows the importance of ABA as a central regulator and integrator of long-term changes in stomatal behaviour, including sensitivity, elicited by external signals. Understanding this architecture may aid breeding of crops with improved water and nutrient efficiency.

Introduction

Stomata are pores on the leaf surface bounded by two guard cells. Their role is to optimize gas exchange in changing environmental conditions[1-3]. In the light, stomata open, allowing CO_2 to enter the leaf for photosynthesis. In contrast, darkness, high concentrations of CO_2, reductions in RH which is equivalent to an increase in the water vapor pressure deficit (VPD) and exposure to the hormone abscisic acid (ABA) promote stomatal closure[4-8]. This is a rapid process typically lasting from 20 – 40 minutes. Reductions in stomatal aperture are the result of turgor and volume reduction in the respective guard cell pair. The key player in ABA- and CO_2-dependent guard cell deflation is the guard cell anion channel SLAC1 together with the SLAC1-activating protein kinase OST1[9]. Under low, sub-threshold concentrations of ABA, the protein phosphatase ABI1 keeps the guard cell anion channel kinases dephosphorylated and SLAC1 inactive[10]. When the concentration of ABA increases it binds to receptors of the PYL/PYR/RCAR family[11-13]. ABA-receptor interaction prevents the ABI1-mediated inactivation of the SLAC1 kinase. This results in anion channel opening, which in turn brings about depolarization of the plasma membrane. The change in membrane potential results in the release of osmotically active K^+ and anions. This is followed by osmotic water release causing guard cells deflation and stomatal closure[4,9,14,15].

Over the last 40 years most investigations have concentrated on identifying and understanding how individual guard cell proteins and intracellular second messengers interact to bring about these rapid changes in stomatal aperture. In contrast, we know much less about the processes that underlie stomatal acclimation to longer term environmental changes[16]. These involve alterations in gene expression, which result in changes in stomatal development and function. In the former category it is recognized that plants acclimate to increases in the concentration of atmospheric carbon dioxide and light intensity by decreasing the number or size of stomata that develop on the surface of plant leaves[17-21]. Reducing stomatal density is known to increase plant water use efficiency[22]. Stomata also acclimate to changing environments by altering their sensitivity to ABA. In Arabidopsis this happens during development with the youngest guard cells being ABA insensitive[23]. Guard cell sensitivity to ABA is modulated by water stress or exposure to increased VPD[23,24]. In these cases, “switching on” ABA responsiveness provides the plant with the ability to control its water relations.

Understanding how stomata acclimate to changes in their environment has clear relevance to the global challenge of producing crops that are more resilient to environment change. Here we identify changes in guard cell gene expression that are likely to contribute to the mechanisms that allow stomatal aperture responses to adapt in the longer term to changes in closure-inducing environmental signals. We reveal that these responses are characterised by the expression of both stimulus-specific suites of genes and core genetic modules that are regulated by all closure-inducing stimuli. We also suggest that part of stomatal acclimation to all these signals is achieved by controlling the sensitivity of the guard cell to ABA. This is achieved by differentially regulating the expressions of members of the PYR/PYL/RCAR family of

ABA receptors. Moreover, we show, in the cases of ABA and elevated CO_2, that response specificity is achieved by these signals accessing different members of the PYR/PYL/RCAR family of receptors.

Stimulus-specific modulation of guard cell gene expression.

To investigate the effects of ABA, low air humidity / increased VPD, darkness, and elevated CO_2 on guard cell gene expression we used a microarray-based approach. We reanalysed two microarray data sets (ABA and RH / VPD treatment) from a previous study[6] and combined them with two new microarray studies where we used darkness and high CO_2 as stomatal closing signals (for detailed analysis of the differentially expressed genes see Supplementary Table 1a). We first analysed the resulting data set using classical pathway analyses and this revealed that each closure-inducing signal addressed a defined, unique cluster of gene pathways (Fig. 1, Supplementary Fig. 1a and Supplementary Information 1). We also found that gene clusters are shared among two, three or all four stimuli. For example, the shared clusters for ABA and lowered RH (equivalent to increased VPD) are dominated by the ABA response (Supplementary Fig. 1b) and the LEA pathways and are up-regulated by both treatments. To gain further information about the interrelationship of these pathways we analysed the co-expression patterns of the genes from each pathway using the public ATTED II database[25]. This analysis revealed that both pathways are highly interconnected (Supplementary Fig. 1c to e). Notably, *RAB18*, *DAA1* and *MYB74*, which we had previously identified as being core to RH (VPD) and ABA induced guard cell responses[26] were co-expressed with

several other genes common to both responses, such as the dehydrins and members of the *HVA22* family (Supplementary Fig. 1c to e).

The shared gene cluster of darkness and low RH (high VPD) is dominated by abiotic stress and glucosinolate pathway genes. Both clusters contain flavin monoxygenases/glucosinolate oxygenases (*FMOGS*), which are responsible for the last step of side chain modification of aliphatic glucosinolates. *FMOGS* are involved in biotic and abiotic stress responses in general and most of them are induced by ABA[27]. The shared cluster for darkness/CO_2, ABA/darkness, ABA/CO_2 and RH/CO_2 are dominated by more general metabolic pathways, receptor kinases, cell wall degradation, major carbohydrate metabolism, glucosidases and transport (Supplementary Fig. 1a). To directly model these complex interconnections, we performed an integrative network analysis based on a rigorous mathematical approach (see Material and Methods).

Specifically, we incorporated the set of protein-protein interactions from the STRING database, which primarily represents physical interactions between proteins, into our analysis. By integrating these data we add a new dimension into the expression data. In contrast to the co-expression network, this allows the detection of functional signalling links at the post-translational protein level. We analysed the network on the basis of the measured expression levels into functionally coherent modules. These can be regarded as the building blocks of cellular processes, such as basic signalling cascades. The resulting optimal solutions represent maximally responsive network modules with respect to the specific experimental stimuli.

This approach is hypothesis free and allows an unbiased exploration of stimulus-triggered network responses, and in particular can integrate novel, hitherto unknown,

genes and connections into a pathway. Based on this algorithm we were able to expose clusters and connections, which cannot easily be detected by classical methods. This revealed stimulus-specific gene modules responsive to different stomata closing signals (Fig. 2a-d) (for details see Supplementary Information 2, Supplementary Table 1b and Supplementary Fig. 2a-d).

Closure-inducing signals differentially modulate PYR/PYL/RCAR receptor expression.

Another feature to emerge from our investigations was that the different closure-inducing signals led to differential expression of ABA receptor family members in guard cells. At the level of the whole plant and at the tissue level it has been documented that ABA application regulates the expression of certain PYR/PYL/RCAR receptors[13,28]. In our investigations we found that six guard-cell-localized *PYR/PYL/RCARs* were affected (Fig. 2e). In the case of ABA, three receptors (*PYL2, 4,* and *5*) were down-regulated while darkness up-regulated *PYR1*. Exposure to dry air (increased VPD) resulted in the downregulation of *PYR1, PYL2, 4,* and *8*. In high CO_2, *PYL8* is up-regulated while *PYL2* is down-regulated. These data suggest that ABA and receptors of the *PYR/PYL/RCAR* family are involved in the response to all these closure-inducing stimuli. One possible interpretation of these results is that, in the long term, acclimation to these signals is achieved through modulating the transcript abundance of individual *PYR/PYL/RCAR* family members. The net result of this would be to fine-tune guard cell sensitivity to ABA. In this context it is interesting that we found that transcript abundance for these receptors was differentially sensitive to ABA concentration. Specifically, we observed that 250 nM ABA induced a reduction in *PYL4* abundance while changes in the

abundance of *PYL2, 4, 5, 8,* and *PYR1* were only observed on treatment with 10X this concentration of ABA (2.5uM). In this context, it should be mentioned that the products of ABA metabolism might interact with ABA receptors. This is indeed the case for phaseic acid that is capable of binding to PYL2[29]. It is therefore possible that these metabolic products could also regulate transcriptional changes of the receptor genes. We next investigated whether other guard cell ABA-regulated genes were, like the *PYR/PYL* genes, differentially regulated in a concentration-dependent manner. As is apparent from the data in Table 1 and Supplementary Fig. 3 (see for details and statistics), *ABR, HAI1* and *MYB60* responded to ABA stimulation in a concentration dependent manner. Together, these observations suggest a framework in which ABA regulates specific receptor family member abundance in a concentration dependent manner. This would potentially provide a high degree of control over receptor and response sensitivity.

Differential guard cell gene expression regulated by PYR/PYL family members.

We next decided to investigate the possibility that different members of the PYR/PYL/RCAR receptor family differentially regulate gene expression. For this we used Arabidopsis *PYR/PYL/RCAR* receptor mutants. The Arabidopsis genome contains 14 *PYR/PYL/RCARs* and previous studies have shown that generation of quadruple, pentuple and sextuple mutants is required to obtain robust ABA-insensitive phenotypes[12,28,30]. However, both biochemical analyses of different receptor-phosphatase complexes and receptor gene expression patterns suggest that the function of ABA receptors is not completely redundant [28,31,32]. Analysis of the single *pyl8* mutant, for example, has revealed a non-redundant role of PYL8 in root sensitivity to ABA[33,34], while the PYL9/RCAR1 receptor specifically regulates the

protein phosphatase AHG1[32] and promotes leaf senescence[35]. Additionally, a non-redundant function of the dimeric receptor BdPYL1 has been reported in Brachypodium[36]. Functional diversification follows the evolutionary expansion of a gene family, therefore we investigated the role of different ABA receptors in guard cells.

Our transcriptomic data confirmed that guard cells express the six ABA receptors *PYR1, PYL1, 2, 4, 5, and 8* that have previously shown to be relevant for stomatal closure[7,28]. We therefore asked whether, in guard cell ABA signalling, the six different receptors are redundant or if each *PYR/PYL* has individual functions. To answer this question, we used the *pyr/pyl* quintuple mutant known as 12458[28], where the receptors *PYR1* and *PYL2, 4, 5, 8* are knocked out and the 11458[33] loss of function mutant in which *PYR1* and *PYL1, 4, 5, 8* are knocked out. In addition, we took advantage of the availability of quintuple mutant complementation lines. These lines under the control of the guard cell specific GC1 (At1g22690) promoter[37] express single receptors individually (see details in Supplementary Fig. 4).

To exclude the possibility that the following results were influenced by overexpression of the individual receptors in the complementation lines, we measured the expression levels of *PYR1, PYL1, PYL2, PYL4, PYL5* and *PYL8* in guard cells of wildtype, both quintuple mutants and the complementation lines in the 12458 background (Supplementary Fig. 5a-f). These results showed that neither *PYL1* (present in 12458) nor *PYL2* (present in 11458) were up-regulated in the quintuple mutants to compensate for the lack of the ABA receptors that were knocked out. Furthermore, the complementation lines showed wildtype-like

expression of the respective receptors (maximally varying about 2-3fold). To confirm that ABA receptor RNA abundance is mirrored on protein level, we selected PYL2 as test case for a mass-spectrometry-based proteomic approach, because PYL2 is the most relevant for ABA induced stomatal closure (see below). As expected PYL2 receptor peptides were neither found present in the 12458 mutant nor the associated PYR1, PYL4 und PYL5 complementation lines. In wildtype guard cells and those of the PYL2 complemented 12458 mutant, however, PYL2 peptides were detected at comparable levels (Supplementary Fig. 5g). These findings underline the suitability of the GC1 promoter to drive nearly guard cell physiological ABA receptor expression.

To resolve whether different members of the PYL/PYR receptor family regulated expression of guard cell genes in a differential fashion we concentrated on the ability of ABA to regulate the following known guard cell ABA-responsive genes, *MYB60, ABI1, ABI2, CIPK25 and KCR2*[6] (Table 2 and Supplementary Fig. 6 for details and statistics). We observed *MYB60* downregulation in wildtype, and 11458 (*PYL2* present) but not in 12458 (*PYL1* present) mutant. Complementation of the latter mutant with *PYR1* or *PYL2* restored the wildtype-phenotype, indicating that ABA-dependent down-regulation of *MYB60* is under control of these receptors. Up-regulation of ABI2 expression was abolished in 11458 but it was restored by PYR1 or PYL1 complementation, indicating that *PYR1* and *PYL1* are sufficient for *ABI2* expression. Likewise, up-regulation of CIPK25 was abolished in 11458 but restored by *PYL1* or *PYL8*, indicating they are sufficient for *CIPK25* expression. A complex regulation of KCR2 expression seems to occur since ABA-induced upregulation was abolished in 11458 (*PYL2* present) and could not be restored in complementation lines. Finally, although RAB18 appeared to be always induced by ABA, the presence

of PYL1 in the 12458-mutant (pval 0,00018) or combined with PYR1 (pval 0,025) led to 12 to 14fold induction (more than threefold of the wt), but when just one of the receptors PYL2, 4, 5 was expressed, this over-induction was suppressed. Since we found no strong differences in the basal levels of the examined genes in the different genetic backgrounds (Supplementary Table 1c), these findings indicate that transcriptional guard cell ABA responses are mediated by individual receptors or distinct *PYR/PYL* combinations.

Loss of PYL2 gene renders stomata ABA insensitive

The above experiments reveal the role of individual PYR/PYL family ABA receptors in the control of guard cell gene expression. We next turned our attention to investigating whether individual receptor family members have distinct roles to play in the control of stomatal aperture and gas exchange. To do this we first used infrared gas analysis (IRGA)[38]. In this approach we used excised leaves and applied ABA via the petioles to exclude any root-effects on transpiration. Under these conditions wild-type leaves opened their stomata upon illumination and adjusted their aperture to the environmental settings prior to ABA application[39]. We found that in the light, the 12458 quintuple mutant (*PYL1* present) in contrast to the 11458 mutant (*PYL2* present) exhibited a severe open-stomata phenotype that manifested itself in rapid wilting on exposure to light. To overcome this experimental difficulty, we pre-incubated plants in the dark with 25 µM ABA for 1h hour before applying the light stimulus. Using this protocol, upon illumination wildtype plants remained in a non-transpiring state (that is ABA inhibited light-induced stomatal opening). In contrast, transpirational water loss of the ABA insensitive 12458 mutant increased over time

(Fig. 3a), whereas the 11458-quintuple mutant, which expressed wild type *PYL2,* behaved almost like wildtype (Fig. 3a). Thus, we tested all available complementation lines in the 12458-background. The 12458-mutant, when complemented by *PYR1,* exhibited reduced transpiration, but the presence of *PYR1*, however, did not fully complement the ABA insensitive phenotype of the quintuple mutant that had lost *PYL2* (Fig. 3b). These data suggest a key role for PYL2 in the guard cell ABA signalling pathway that leads to stomatal closure. This was confirmed by complementing *PYL2* in the 12458-mutant which resulted in a plant that showed the same ABA suppression of stomatal transpiration as the wildtype (Fig. 3b). In contrast, guard cell expression of *PYL4* and *5* did not complement the wilty 12458-mutant phenotype (Fig. 3c).

In addition to IRGA measurements, which provide data on, in this case, the effects of manipulating gene expression on stomatal transpirational control at the level of the whole leaf, we followed the response of individual stomata in their natural environment of the intact leaves. This was achieved by applying 50μM +/- ABA (corresponding to 25μM biologically active ABA) to single stoma via micropipette-assisted electro-infusion. By introducing ABA directly to the guard cells we aimed to exclude any indirect hormone effects via, for example, the mesophyll cells and, or vasculature on the control of transpiration by stomata. Using this protocol we observed that stomata of wildtype Arabidopsis closed within 10 min of exposure to ABA (Fig. 4a and b and Supplementary movies). In contrast stomata of the 12458 mutant (*PYL1* present) did not respond to the hormone and remained open. This mutant was also the only one with significantly wider open stomata under control conditions (Fig. 4c). In the quintuple mutant (12458) complemented by *PYL2* and the

11458 mutant (*PYL2* present), we observed stomatal closure that was identical to WT. We also observed that PYL5 was not able to complement the ABA insensitive phenotype (Fig. 4a and b and Supplementary movies). This demonstrates that PYL2 is sufficient to fully rescue guard cell's ABA signalling and fast stomatal closure. To confirm our findings that PYL2 and partially PYR1 are able to complement the ABA insensitivity of the 12458 mutant, we repeated the ABA pre-incubation experiment with the *pyl2-1* loss of function mutant (seed strain GT2864)[12] and the corresponding Ler wildtype. Although PYR1, PYL1, PYL4, PYL5 and PYL8 are present in this mutant, *pyl2-1* behaved almost like the *PYR1* complementation line in the 12458 background (Supplementary Fig. 7), supporting our hypothesis that PYL2 and PYR1 are the key receptors for proper ABA induced stomatal closure.

PYL4 and PYL5 are sufficient for CO_2 -induced stomatal closure

Since Raschke's research in the 1970s we have known that stomata require ABA to sense elevated CO_2[7,8,40,41]. However, the molecular basis of this interaction has not been clear. We took advantage of the panel of ABA receptor mutants previously described to investigate the basis of the interaction using IRGA. Stomata that had been opened in the light in the presence of 400 ppm CO_2 (ambient) were exposed to 1000 ppm CO_2. This resulted, as expected in a decrease in transpiration consistent with reduction in stomatal aperture (Fig. 5a). Next, we used the 11458 mutant in which PYL2 is naturally expressed. We had previously shown that this PYL2 expressing mutant showed wildtype-like ABA-induced closure response (Fig. 3b). However, in contrast to ABA, CO_2-induced closure was impaired in this as well as in the 12458 mutant (Fig. 5a). Stomata of complementation lines in the 12458-background (with PYL1 present) expressing *PYR1* or *PYL2* remained impaired in

their response to high CO_2 as well (Fig. 5b). However, lines that express *PYL4* or *PYL5* in guard cells regained stomatal CO_2 sensitivity similar to wildtype plants (Fig. 5c). These data show that PYL4 or PYL5 are sufficient for the induction of closure by increased CO_2. Interestingly, except the *PYL5* complementation line, all other mutants showed remarkably higher ground levels of transpiration in the light and under ambient CO_2 atmosphere compared to wildtype (Supplementary Fig. 8). Only the *PYL4* complementation line started to reopen their stomata after about 2 h of high CO_2-treatment. Future studies will investigate whether this behaviour represents a phenomenon associated with adaption (Supplementary Fig. 8).

Discussion

The primary objective of the work described in this paper has been to explore how stomata adapt to changed environmental conditions. Our focus has not been on changes in stomatal development induced by changes in the environment. Rather, we have concentrated on examining the mechanisms likely to underpin, changes in, for example, the sensitivity of the stomatal aperture response to closure-inducing stimuli. Specifically, when we looked at 4 different closure-inducing stimuli, we found that they regulated a diverse set of intracellular pathways. While there was some overlap there were marked differences and this must reflect specific effects of these signals on guard cell properties. However, markedly, the integrated network analysis (see Supplementary Information 3) revealed that all closure-inducing signals induced changes in the expression of the *PYR/PYL/RCAR* ABA receptor family. This provides a mechanism for all stimuli to modify stomatal function through modulating the sensitivity of the ABA signalling pathway. We investigated the control of guard cell gene expression by ABA in more detail and found that individual genes, including members of the ABA receptor family, responded to ABA in a concentration

dependent manner. This conclusion was strengthened when we found that the expression in guard cells of *PYL4* or *PYL5* was sufficient for CO_2-induced stomatal closure but was not sufficient to restore the ability of ABA to inhibit light-induced stomatal opening in the 12458 mutant, whereas PYL2 was sufficient for this response. Our data on the ABA response of the complemented lines agree with a previous publication[42] which showed that pyr1/pyl1/pyl2/pyl4 quadruple mutant plants did not close their stomata following ABA application and that ABA preincubation could not prevent stomatal opening by light. In contrast, in another study[43] using the same mutant, ABA application to open stomata did also not induce stomatal closure, but ABA preincubation prevented stomatal opening. In the latter paper the authors used guard cells in epidermal peels (obtained by macerating leaves in a waring blender) floating on ABA solutions. Future studies will have to investigate whether and how mechanical stress feeds back on guard cell ABA biology. It should be noted that *pyl2-1* single mutant[12] behaved like the *PYR1* complemented 12458 plants indicating that PYR1 and PYL2 are the most important receptors for the fast ABA response of guard cells. However, one might not be able to exclude the possibility, that either PYL8 or heterodimers involving receptors other than PYL2, are also competent to rescue the ABA-insensitive phenotype of the 12458 mutant.

In terms of stomatal CO_2-responsivness, a previous report agrees that CO_2-induced induced stomatal closure is disrupted in ABA-receptor mutant backgrounds[8]. In contrast another paper concludes that "rapid CO_2 signal transduction leading to stomatal closure via an ABA-independent pathway"[44]. How might these radically different conclusions be reconciled? It is of course only possible to speculate. However, as documented earlier[23] stomatal responsiveness to ABA varies from

insensitivity to sensitivity and that this is regulated by relative air humidity (VPD). Modulation of stomatal sensitivity by plant growth conditions such as relative humidity could provide a framework to explain the disparity in the results. The veracity of such a possibility requires further experimentation. Nevertheless, it is worth pointing out that examination of the data in Hsu et al.[44], like before in Merilo[7], reveals that the quadruple receptor mutants *pyr1/pyl4/5/8* and hexuple *pyr1/pyl1/2/4/5/8* display reduced CO_2 responsiveness compared with wild type. These data do indicate a role for ABA receptors in the response to CO_2. This was also the conclusion reached when stomatal conductance in response to CO_2 was analysed in wild type and *pyr1/pyl1/2/4/5/8*[7]. Finally, long-term exposures of the in-gel kinase assays done by Hsu et al.[44], showed a basal activity of OST1 in guard cells which, according to the authors, is probably necessary for rapid CO_2-induced stomatal closure. Such basal level of phosphorylation would be very sensitive to phosphatase and PYR/PYL/RCAR activity, which can be modified by nanomolar changes in ABA concentration (K_d for ternary complexes in the 20-40 nM range[11,13]). However, to return to the current investigation, our data, including its in-depth analysis of receptor mutants, are strongly supportive of a role for ABA receptors, in particular PYL4 and PYL5 in the stomatal response to increased concentrations of CO_2.

Together our investigations, reveal not only the complexity of the underlying cellular mechanisms responsible for controlling stomatal responses to closure-inducing signals and how this might contribute towards stomatal response acclimation, but they also reveal a plausible mechanism for how stomata might integrate multiple signals. The results here are likely to be of benefit to plant breeders who are

interested in engineering crops to respond to the complex multiple environmental stresses that are likely to be associated with future climates.

Material and Methods

Plant Material and Growth Conditions

Arabidopsis thaliana plants were grown in soil that was semi sterilized for 20 minutes at 100 ^{o}C and cultivated in climate chambers (Binder KBWF 720; www.binder-world.com) in a 12 h day night rhythm (22/16 ^{o}C, 60% RH) and were illuminated with 125 µmol m^{-2} s^{-1} white light. The gas exchange measurements and the expression studies were performed with 6 to 8 weeks old adult, non-flowering plants.

Preparation of the ABA-receptor mutants

Using Col genomic DNA as template we amplified by PCR the promoter region of At1g22690 located 1716 bp upstream of the start codon, named GC1[37], using the primers FGC1: 5'-ACCATGGAGTAAAGATTCAGTAACCC and RGC1: 5'-ATCCATGGTATTTCTTGAGTAGTGATTTTGAAG. Next GC1 was cloned in pCR8/GW, excised as a NcoI fragment and cloned in front of either PYR1, PYL2, PYL4, PYL5 or PYL8. The resulting pGC1-PYR/PYL construct was recombined by LR reaction into modified pAlligator2[45], which has been previously HindIII-EcoRV doubly digested, treated with Klenow and religated to obtain a construct lacking the 35S promoter. Each modified pAlligator2-*GC1:PYR/PYL* construct was transferred to *Agrobacterium tumefaciens* C58C1 (pGV2260)[46] by electroporation and used to transform 12458 and 11458 mutant plants[28,33] by the floral dip method[47]. T1

transgenic seeds were selected based on seed GFP fluorescence and sowed in soil to obtain the T2 generation. Homozygous T3 progeny was used for further studies. Several *PYL8::12458* complementation lines were also tested but did not grow properly. They showed a severe phenotype and excised leaves wilted immediately. These mutants could not be used in any of our physiological experiments and were thus excluded from our analyses.

Infra-Red-Gas-Analyses (IRGA)

Stomatal closing assays: ABA and low air humidity application were performed as described[6]. In brief, ABA solution (50 µM +/- ABA) was sprayed to the plants until the surface was fully covered. The low humidity treatment was performed by reducing the RH from 80% to 20% at 22°C what equals a VPD change from 0.529 to 2.116 kPa. High CO_2 (1000 ppm) was applied to plants in airtight boxes after two hours illumination at ambient air to close stomata. For the samples in darkness plants were fully shaded following two hours of illumination. Each closing signal persisted for four hours. To minimize diurnal effects on gene expression, all procedures were started in the morning following two hours after onset of illumination.

Leaf gas exchange measurements: Transpiration rates were measured with a custom-made system as described elsewhere[38]. CO_2 response measurements were performed with intact plants at 20°C and 52,5 ± 3% RH (VPD = 1.123 kPa). The soil surface of the pots was tightly covered with plastic foil to avoid water evaporation. After the transpiration rates had stabilized in darkness, plants were illuminated with 125 µmol m^{-2} s^{-1} white light. After 1h of illumination the CO_2-concentration of the air stream was increased from 400ppm to 1000ppm.

448 The effect of ABA on the light induced transpiration of Arabidopsis was measured
449 with detached leaves and the same conditions as described for the CO_2
450 measurements. To avoid xylem embolism, the leaves were cut under water. The
451 petioles were directly transferred into 50 µM +/- ABA solution and incubated in
452 darkness. After one hour ABA incubation leaves were illuminated with 125 µmol m^{-2}
453 s^{-1} white light and the transpirational water loss was recorded.
454
455 **ABA Electro-Infusion**
456 This method was performed according to[48]. Excised leaves from 5-6-week-old plants
457 were attached to a petri dish using double-sided tape and submerged in a bath
458 solution (1mM KCl, 1mM $CaCl_2$ 5mM MES/BTP, pH 6). The petri dish was mounted
459 to an upright microscope (Axioskop 2FS, Zeiss, Jena, Germany) and the leaves were
460 left for incubation while being exposed to 125 µmol m^{-2} s^{-1} light. Stomata on the
461 leaves abaxial side were visualized with a water immersion objective (Achroplan
462 x63/0.9 W, Zeiss) and images were recorded with a camera (CoolSNAP HQ, Visitron
463 Systems, Puchheim, Germany) in 30 sec intervals using VisiView (Visitron Systems)
464 imaging software. Electrodes from borsilicat capillaries (inner/outer diameter =
465 0.56/1.0 mm; Hilgenberg, Malsfeld, Germany) were pulled on a horizontal laser puller
466 (P2000, Sutter Instrument, Novato, CA, USA) to achieve resistances ranging from 60
467 to 100 MΩ. The electrodes were tip-loaded with 50 µM +/- ABA, backfilled with 300
468 mM KCl and connected by Ag/Ag half cells to the head stage (HS-2A x 0.01; Axon
469 Instruments, Molecular Devices, Sunnyvale, CA, USA) of a TEVC amplifier
470 (GeneClamp 500; Axon Instruments). Reference electrodes were prepared using
471 capillaries filled with 300 mM KCl, sealed with an agar plug (2 % w/v agarose, 300
472 mM KCl and connected to ground with an Ag/Ag half-cell). Microelectrodes were

driven with a piezo-electric micromanipulator (MM3A; Kleindiek, Reutlingen, Germany). Prior to electro-infusion the electrode was brought in close proximity to an open stoma and left for 10 min to ensure no mechanical closing stimulus was applied. ABA or control solution was released from the capillary by a negative 10 min, 1 nA current-puls. After additional 10 min the image recording was stopped.

ABA spray experiments

Arabidopsis plants were ABA treated via spraying until leaves were moist. To investigate the dose dependency of the ABA receptor expression in wildtype plants, ABA solutions with 0 (control plants) 0.025, 0.1, 0.25, 2.5 and 25 µM ABA in deionised water containing 1:10000 Triton-X100 were used. To investigate ABA regulated guard cell expression patterns, plants were sprayed with 25 µM ABA solution or deionised water with Triton-X100. After 4h of incubation guard cells were sampled and RNA was extracted.

CO_2 treatment for microarrays

Single potted 6-7 week old *Arabidopsis thaliana* (Col 0) plants were subjected to an airstream containing ambient CO_2 (380ppm) and 50 ± 5% RH (VPD = 1.322 kPa) in climate chambers at 22 ± 2 °C and 100 µmol m-2 sec-1 white light. After 1h half of the plants were treated with 1000 ppm CO_2 for 4h. Guard cells were sampled and RNA was extracted for microarray hybridisation.

Darkness treatment for microarrays

Single potted 6-7 weeks old *Arabidopsis thaliana* (Col 0) plants were subjected to an airstream containing ambient CO_2 (400ppm) and 50 ± 5% RH (VPD = 1.322 kPa) in

498 climate chambers at 22 ± 2 °C and 100 µmol m-2 sec-1 white light. After 2 h half of
499 the plants were kept into darkness for 2 h. Guard cells were sampled and RNA was
500 extracted for microarray hybridisation.
501
502 **ABA and low RH (increased VPD) treatment**
503 These microarray data come from a previous study[6] in which the ABA and low
504 humidity (increased VPD) signals persisted over 4 hours.
505
506 **Sampling and RNA Extraction**
507 Guard cell sampling and RNA extraction were performed as described[6]. Guard cell
508 samples were frequently tested via vital staining to confirm that contaminations by
509 other cell types remained below 5%–10%.
510
511 **Quantitative Real-Time PCR**
512 Quantitative real-time PCR (qPCR) was performed as described[49]. All transcripts
513 were normalized to 10,000 molecules of actin2/8 and thus denoted as relative
514 expression. All indicated replicate numbers refer to biological replicates. Primer
515 sequences used: PYR1fwd 5'-GCTGACGAATTACAAATCCGTT-3',
516 PYR1rev 5'-ACCGTCGCGAGTTTCTG-3', PYL1fwd 5'-CGTGAACGTGATAAGTGG-
517 3', PYL1rev 5'-TGAACCGTCGTAACCGAT-3',
518 PYL2fwd 5'-CATAACCCAACGCATCCA-3', PYL2rev 5'-AACTCAAGCCGCTCGGTA-
519 3', PYL4 fwd 5'-CCGCTCGTTTTCACACACAC-3', PYL2rev 5'-
520 GTGTTGCCTGGAGGAACATC-3', PYL5fwd 5'-TGGTGCAGATGATCCACG-3',
521 PYL4rev 5'-AGACTGAAGGTTGCACCG-3', PYL8fwd 5'-TGTGTGGTCACTTGTGAG-
522 3', PYL8rev 5'-TGAACCGCAAGACGTTCA-3',

KCR2fwd 5'-ATGTGGATGCACTATCA-3', KCR2rev 5'-AAGGTTATCCGGTACAA-3', ABI2fwd 5'-GGACTTAGAGGCTATTG-3', ABI2rev 5'-AGGATTAAATCCATTAGTG-3', MYB60fwd 5'-ATGCTGTGACAAGATAGG-3', MYB60rev 5'-AAAGTTTCCACGTTTAAT-3' CIPK25fwd 5'-AGATCCAAAACGTAGAAG-3', CIPK25rev 5'-CTTACACAACTCAACGAC-3', HAI1fwd 5'-GTTGAATAGTTTTGACGA-3', HAI1rev 5'-GCCGTATTTAGGATAAGC-3', ABRfwd 5'-GGTGGAATGATGGACAAG-3', ABRrev 5'-ATAAAGATCCAAATGGACG-3', RAB18fwd 5'-AGAAGGGAATAACACAAA-3', RAB18rev 5'-CAATACAACGACCGAA-3'.

PYL2 protein identification

For the identification and quantification of PYL2, parallel reaction monitoring (PRM) via mass spectrometry was used. Four or five biological replicates from each experimental group were examined. Proteins were extracted from the ground GCs following the phenol extraction/ammonium acetate precipitation method described[50]. Briefly: 150 mg starting material was processed. For tryptic digestion, an aliquot of 20 µg protein was digested with 0.2 µg trypsin. Samples were cleaned using C18 solid phase extraction according to the manufacturer (Pierce™ C18 Spin Columns, Thermo Fisher Scientific, Gent, Belgium) and dissolved in 5% ACN, 0.1% formic acid. Peptides from the candidate proteins were designed using Skyline (version 4.2) and ordered from Thermo Fisher Scientific (UK) (PEPotec Grade 1). The ultra performance liquid chromatography - tandem mass spectrometer (UPLC–MS/MS) analysis was performed an Ultimate 3000 UPLC system (Dionex, Thermo Scientific) equipped with a C18 PepMap100 precolumn (5 µm, 300 µm × 5 mm, Thermo Scientific) and an EasySpray C18 column (3 µm, 75 µm × 15 cm, Thermo Scientific)

548 using a gradient of 5% to 20% ACN in 0.1% formic acid (FA) for 10 min followed by a
549 gradient of 10% to 35% ACN in 0.1% FA for 4 min and a final gradient from 35% to
550 95% ACN in 0.1% FA for 2.5 min and a Q Exactive Orbitrap mass spectrometer
551 (Thermo Scientific, USA). The flow-rate was set at 250 µl/min. The Q Exactive was
552 operated in a positive ion mode with a nanospray voltage of 1.5 kV and a source
553 temperature of 250 °C. ProteoMass LTQ/FT-Hybrid ESI Pos. Mode CalMix
554 (MSCAL5-1EA SUPELCO, Sigma-Aldrich) was used as an external calibrant and the
555 lock mass 445.12003 as an internal calibrant. For the characterization of the
556 standard peptide library, the instrument was operated in a data-dependent
557 acquisition mode with a survey MS scan at a resolution of 70,000 (FWHM at m/z
558 200) for the mass range of m/z 350–1800 for precursor ions, followed by MS/MS
559 scans of the top 10 most intense peaks with + 2, + 3 and + 4 charged ions above a
560 threshold ion count of 16,000 at a 35,000 resolution using a normalized collision
561 energy (NCE) of 28 eV with an isolation window of 3.0 m/z and dynamic exclusion of
562 10 s. All data were acquired with Xcalibur 2.2 software (Thermo Scientific). The most
563 suitable peptide per protein was chosen to set the PRM analysis. To avoid
564 overlapping time windows the samples were analysed on the QE in PRM mode in 2
565 separate runs.
566

Peptide Name	Sequence	Peptide Length	m/z	Z	Start	End	Run
PYL2	LISGDGDVGSVR	12	587,8068	2	25,9	28,9	1

567
568 PRM analysis was performed in Skyline 4.2. The dicyano-1,4-benzoquinone (DDQ)
569 analysis of the peptide library was analysed with proteome discoverer and the library
570 was loaded in Skyline as a msf file. The NCBI Arabidopsis fata file was loaded and

571 the results of the PRM run were loaded as raw files with the following settings: MS1
572 orbitrap detection 70 000 resolution MS2 orbitrap detection 20 000 resolution. Only
573 peptides showing 3 accurate transitions were accepted.

574 **Microarray Hybridization**

575 For transcriptome profiling samples were hybridized on an Agilent Platform using the
576 Agilent *Arabidopsis* V4 (design number 021169) microarray chips
577 (http://www.agilent.com). RNA quantity was measured with a ND-100
578 Spectrophotometer v3.3.0 (NanoDrop Technologies). RNA integrity was confirmed
579 using an Agilent RNA 6000 Nano Chip on an Agilent 2100 BioAnalyzer (vB.02.03
580 BSI307). 500 ng total RNA were used for each sample labeling. Labeling and
581 preparation of samples for hybridization was performed as described in the one-color
582 microarray-based gene expression analysis protocol provided by Agilent including
583 the one-color RNA spike-in kit (v5.0.1, 2006; Agilent Technologies, Santa Clara).
584 Slides were scanned on the Agilent Microarray Scanner with extended dynamic
585 range (XDR) at high resolution (5 µm). Data sets were extracted by propriety
586 software package (v9.5.3.1/ Agilent Technologies) using a standard protocol.

587

588 **Array Analysis**

589 Data preprocessing was performed using the Bioconductor software[51] with the
590 statistical programming environment R[52]. Normalization has been performed using
591 negative control probes and quantile normalization using negative and positive
592 control probes as implemented in the neqc function[53] of the Limma package[54].
593 Differential gene expression for all stimuli was calculated using the moderated t-
594 statistic approach as implemented in the R-package Limma[54], which has been
595 specifically developed for the analysis of small sample size experiments. The p-

values of all results were corrected for multiple testing by using the false discovery rate (FDR)[55]. In order to identify guard cell specific gene regulation, we used a meta-analysis approach based on the order statistic of the stimulus p-values. Therefore, p-values from a one-sided moderated t-test of differential expressed genes between guard cells and leaf tissue have been derived from the Limma model. Subsequently, for each stimulus a combined p-value has been calculated using the second order statistics of the stimulus and the guard cell versus leaf p-value. This results in a set of genewise p-values for guard cell specific stimulus effects.

Pathway enrichment Analyses

Analysis was carried out by a model-based approach which can directly be integrated into the Limma analysis of differential expression. A competitive gene set test has been applied to all stimulation contrasts as implemented in the function camera[56]. This function tests whether a set of genes is highly ranked relative to other genes in terms of differential expression, accounting for potential inter-gene correlation. Pathways for the analysis have been obtained from the MapMan catalogue[57] based on TAIR version 10 (2012), from which all gene sets with more than 5 genes and fewer than 500 genes have been included in the analysis.

Integrative Network Analysis

Network data has been obtained from the STRING database (version 9.0, http://string-db.org)[58]. All interactions of the genome of Arabidopsis *thaliana* have been extracted from the database yielding a total of 717,810 interactions between 16,465 genes. For the analysis we used the high confidence network (combined score > 0.7) resulting in 69,603 interactions between 7,090 genes. After mapping all

genes on the array to the network the resulting largest connected component comprising 69,329 interactions between 6,724 genes has been extracted. This constitutes the base network used in all subsequent network analyses.

An optimal algorithm has been established to decompose the large intricate network structure into functionally coherent network modules[59]. These modules can be viewed as building blocks of cellular processes, such as basic metabolic pathways or stimuli-specifc signalling. To identify these signalling sub networks the genes (network nodes) need to be scored according to their measured regulation and responsive modules can be identified using and exact search algorithm.

Here a statistical model to derive functional scores of closing signal responsiveness in guard cells has been used. Therefore, all stimuli p-values have been derived from the Limma analysis as detailed above. Integrated network analysis node (gene) scores have been computed based on these p-values as detailed in[59] using the routines implemented in the R-package BioNet[60]. Briefly, a Beta-uniform mixture model (BUM) has been fitted to the p-value distribution, thereby decomposing the signal and noise components of the distribution. Based on this, network scores have been calculated as log likelihood ratio of the signal to the noise component. Thus, positive scores reflect signal content (low p-values) whereas the negative scores reflect non-significant genes (noise). The signal to noise threshold has been multiple testing adjusted using the FDR. For the different stimuli appropriate FDR values have been selected according to the different effect strengths controlling the size of the resulting modules. These mainly contain either genes with a maximal response, but also a few tightly associated genes that show no differential regulation on the transcriptomic level (represented as squares in the network). Subsequently, an

exhaustive network search has been performed on the entire node-scored network to identify the maximum scoring sub networks using an exact algorithm[59]. The resulting optimal solutions represent maximally significant differentially regulated modules. Based on the functional scoring of stimulation this constitutes the optimal responsive modules within the entire network. This also means that no other module shows a stronger guard cell-specific closing signal response.

Statistics

To test significances on qPCR (Supplementary Figs. 3, 6 and related Tables 1, 2) we used a multivariable linear model on log transformed expression values (relative to actin) adjusting additionally for day of experiment. Heteroscedasticity-consistent (HC) standard errors for regression coefficients have been calculated as implemented in sandwich package using default setting[61]. For dose response experiments (Supplementary Fig. 3) comparisons of different concentrations to the unstimulated control have been multiple testing corrected based on Dunnet's Post hoc test procedure for many-to-one comparisons. We used the step down adjustment (method="free") as implemented in the 'multcomp' package in R[62]. Reported p-values are based two-sided tests, p-values < 0.05 have been regarded as significant. Levels of significance were * $p \leq 0.05$, ** $p \leq 0.01$, *** $p \leq 0.001$.

Data availability

The data that support the findings of this study are available from the corresponding authors upon reasonable request. Microarray data of the ABA and low air humidity treatments which were taken from[6] were deposited in the Gene Expression Omnibus

(GEO) database http://www.ncbi.nlm.nih.gov/geo with accession no. GSE41054. The microarray data from CO_2 and darkness experiments were deposited at the same database under GSE118520.

Code availability

Algorithms and statistics used in the analyses are based on published approaches available in R packages (mainly Bioconductor framework) and other cited public available repositories.

Corresponding authors

Correspondence and requests for materials should be addressed to A.M.H. and T.M.

Acknowledgements

Work in the Hedrich laboratory was supported by a grant from King Saud University Deanship for Scientific Research, International Research Group Program (IRG14-22), Riyadh, Saudi Arabia and that of the Rodriguez laboratory was supported by the Ministerio de Ciencia e Innovacion, Fondo Europeo de Desarrollo Regional and Consejo Superior de Investigaciones Cientificas (grants BIO2014-52537-R and BIO2017-82503-R to P.L.R.). Marcus Dittrich was supported by the CRC/Transregio 124 – FungiNet funded by the Deutsche Forschungsgemeinschaft (project B2). Alistair Hetherington acknowledges support from the UK BBSRC (Grant No. BB/N001168/1).

Author contributions

M.D. and T.M. conceived and conducted bioinformatics. H.M.M., H.B. and P.A. conceived, performed and analysed the expression studies. H.M.M. conducted and

analysed gas exchange measurements. M.P.L. and P.L.R. conceived and conducted the generation of transgenic plants. C.M.G. and S.C.C. conceived and conducted proteomic analyses. J.H. conceived, conducted and analysed electro infusion experiments. P.A., P.L.R., H.K., K.A.S.A.-R., T.M., A.M.H. and R.H. designed and conceived the study. M.D., T.M., P.A., A.H.M. and R.H. wrote the manuscript. All authors discussed the results and commented on the manuscript.

Competing interests

The authors declare no competing financial interests.

References

1 Hetherington, A. M. & Woodward, F. I. The role of stomata in sensing and driving environmental change. *Nature* **424**, 901-908, doi:10.1038/nature01843 (2003).

2 Vialet-Chabrand, S. R. M. *et al.* Temporal Dynamics of Stomatal Behavior: Modeling and Implications for Photosynthesis and Water Use. *Plant Physiol* **174**, 603-613, doi:10.1104/pp.17.00125 (2017).

3 Lawson, T. & Blatt, M. R. Stomatal size, speed, and responsiveness impact on photosynthesis and water use efficiency. *Plant Physiol* **164**, 1556-1570, doi:10.1104/pp.114.237107 (2014).

4 Assmann, S. M. & Jegla, T. Guard cell sensory systems: recent insights on stomatal responses to light, abscisic acid, and CO2. *Curr Opin Plant Biol* **33**, 157-167, doi:10.1016/j.pbi.2016.07.003 (2016).

5 Engineer, C. B. *et al.* CO2 Sensing and CO2 peculation of Stomatal Conductance: Advances and Open Questions. *Trends Plant Sci* **21**, 16-30, doi:10.1016/j.tplants.2015.08.014 (2016).

6 Bauer, H. *et al.* The stomatal response to reduced relative humidity requires guard cell-autonomous ABA synthesis. *Curr Biol* **23**, 53-57, doi:10.1016/j.cub.2012.11.022 (2013).

7 Merilo, E. *et al.* PYR/RCAR Receptors Contribute to Ozone-, Reduced Air Humidity-, Darkness- and CO2-Induced Stomatal Regulation. *Plant Physiol* **162**, 1652-1668, doi:10.1104/pp.113.220608 (2013).

8 Chater, C. *et al.* Elevated CO_2-Induced Responses in Stomata Require ABA and ABA Signaling. *Curr Biol* **25**, 2709-2716, doi:10.1016/j.cub.2015.09.013 (2015).

9 Hedrich, R. & Geiger, D. Biology of SLAC1-type anion channels - from nutrient uptake to stomatal closure. *New Phytol* **216**, 46-61, doi:10.1111/nph.14685 (2017).

10 Scherzer, S., Maierhofer, T., Al-Rasheid, K. A. S., Geiger, D. & Hedrich, R. Multiple calcium-dependent kinases modulate ABA-activated guard cell anion channels. *Mol Plant* **5**, 1409-1412, doi:10.1093/mp/sss084 (2012).

11 Ma, Y. *et al.* Regulators of PP2C phosphatase activity function as abscisic acid sensors. *Science* **324**, 1064-1068, doi:10.1126/science.1172408 (2009).

12 Park, S. Y. *et al.* Abscisic acid inhibits type 2C protein phosphatases via the PYR/PYL family of START proteins. *Science* **324**, 1068-1071, doi:10.1126/science.1173041 (2009).

13 Santiago, J. *et al.* Modulation of drought resistance by the abscisic acid receptor PYL5 through inhibition of clade A PP2Cs. *Plant J* **60**, 575-588, doi:10.1111/j.1365-313X.2009.03981.x (2009).

14 Munemasa, S. *et al.* Mechanisms of abscisic acid-mediated control of stomatal aperture. *Curr Opin Plant Biol* **28**, 154-162, doi:10.1016/j.pbi.2015.10.010 (2015).

15 Hedrich, R. Ion channels in plants. *Physiol Rev* **92**, 1777-1811, doi:10.1152/physrev.00038.2011 (2012).

16 Franks, P. J., Leitch, I. L., Ruszala, E. M., Hetherington, A. M. & Beerling, D. J. Physiological framework for adaptation of stomata to CO_2 from glacial to future concentrations. *Philosophical Transactions of the Royal Society B: Biological Sciences* **367**, 537-546 (2012).

17 Woodward, F. I. Stomatal Numbers Are Sensitive to Increases in Co2 from Preindustrial Levels. *Nature* **327**, 617-618, doi:DOI 10.1038/327617a0 (1987).

18 Gray, J. E. *et al.* The HIC signalling pathway links CO_2 perception to stomatal development. *Nature* **408**, 713-716, doi:10.1038/35047071 (2000).

19 Doheny-Adams, T., Hunt, L., Franks, P. J., Beerling, D. J. & Gray, J. E. Genetic manipulation of stomatal density influences stomatal size, plant growth and tolerance to restricted water supply across a growth carbon dioxide gradient. *Philos T R Soc B* **367**, 547-555, doi:10.1098/rstb.2011.0272 (2012).

20 Casson, S. A. *et al.* phytochrome B and PIF4 Regulate Stomatal Development in Response to Light Quantity. *Current Biology* **19**, 229-234, doi:10.1016/j.cub.2008.12.046 (2009).

21 Casson, S. A. & Hetherington, A. M. phytochrome B Is required for light-mediated systemic control of stomatal development. *Curr Biol* **24**, 1216-1221, doi:10.1016/j.cub.2014.03.074 (2014).

22 Franks, P. J., T, W. D.-A., Britton-Harper, Z. J. & Gray, J. E. Increasing water-use efficiency directly through genetic manipulation of stomatal density. *New Phytol* **207**, 188-195, doi:10.1111/nph.13347 (2015).

23 Pantin, F. *et al.* Developmental Priming of Stomatal Sensitivity to Abscisic Acid by Leaf Microclimate. *Current Biology* **23**, 1805-1811, doi:10.1016/j.cub.2013.07.050 (2013).

24 Aliniaeifard, S. & van Meeteren, U. Can prolonged exposure to low VPD disturb the ABA signalling in stomatal guard cells? *J Exp Bot* **64**, 3551-3566, doi:10.1093/jxb/ert192 (2013).

25 Obayashi, T., Nishida, K., Kasahara, K. & Kinoshita, K. ATTED-II updates: condition-specific gene coexpression to extend coexpression analyses and applications to a broad range of flowering plants. *Plant Cell Physiol* **52**, 213-219, doi:10.1093/pcp/pcq203 (2011).

26 Bauer, H. *et al.* How do stomata sense reductions in atmospheric relative humidity? *Mol Plant* **6**, 1703–1706, doi:10.1093/mp/sst055 (2013).

27 Kong, W. *et al.* Two Novel Flavin-Containing Monooxygenases Involved in Biosynthesis of Aliphatic Glucosinolates. *Front Plant Sci* **7**, 1292, doi:10.3389/fpls.2016.01292 (2016).

28 Gonzalez-Guzman, M. *et al.* Arabidopsis PYR/PYL/RCAR receptors play a major role in quantitative regulation of stomatal aperture and transcriptional response to abscisic acid. *Plant Cell* **24**, 2483-2496, doi:10.1105/tpc.112.098574 (2012).

29 Weng, J. K., Ye, M., Li, B. & Noel, J. P. Co-evolution of Hormone Metabolism and Signaling Networks Expands Plant Adaptive Plasticity. *Cell* **166**, 881-893, doi:10.1016/j.cell.2016.06.027 (2016).

30 Zhao, Y. *et al.* Arabidopsis Duodecuple Mutant of PYL ABA Receptors Reveals PYL Repression of ABA-Independent SnRK2 Activity. *Cell Rep* **23**, 3340-3351 e3345, doi:10.1016/j.celrep.2018.05.044 (2018).

31 Antoni, R. *et al.* Selective inhibition of clade A phosphatases type 2C by PYR/PYL/RCAR abscisic acid receptors. *Plant Physiol* **158**, 970-980, doi:10.1104/pp.111.188623 (2012).

32 Tischer, S. V. *et al.* Combinatorial interaction network of abscisic acid receptors and coreceptors from Arabidopsis thaliana. *Proc Natl Acad Sci U S A* **114**, 10280-10285, doi:10.1073/pnas.1706593114 (2017).

33 Antoni, R. *et al.* PYRABACTIN RESISTANCE1-LIKE8 plays an important role for the regulation of abscisic acid signaling in root. *Plant Physiol* **161**, 931-941, doi:10.1104/pp.112.208678 (2013).

34 Belda-Palazon, B. *et al.* PYL8 mediates ABA perception in the root through non-cell-autonomous and ligand-stabilization-based mechanisms. *Proc Natl Acad Sci U S A* **115**, E11857-E11863, doi:10.1073/pnas.1815410115 (2018).

35 Zhao, Y. *et al.* ABA receptor PYL9 promotes drought resistance and leaf senescence. *Proc Natl Acad Sci U S A* **113**, 1949-1954, doi:10.1073/pnas.1522840113 (2016).

36 Pri-Tal, O., Shaar-Moshe, L., Wiseglass, G., Peleg, Z. & Mosquna, A. Non-redundant functions of the dimeric ABA receptor BdPYL1 in the grass Brachypodium. *Plant J* **92**, 774-786, doi:10.1111/tpj.13714 (2017).

37 Yang, Y., Costa, A., Leonhardt, N., Siegel, R. S. & Schroeder, J. I. Isolation of a strong Arabidopsis guard cell promoter and its potential as a research tool. *Plant Methods* **4**, 6, doi:10.1186/1746-4811-4-6 (2008).

38 Muller, H. M. *et al.* The desert plant Phoenix dactylifera closes stomata via nitrate-regulated SLAC1 anion channel. *New Phytol* **216**, 150-162, doi:10.1111/nph.14672 (2017).

39 Ache, P. *et al.* Stomatal action directly feeds back on leaf turgor: new insights into the regulation of the plant water status from non-invasive pressure probe

measurements. *Plant J* **62**, 1072-1082, doi:10.1111/j.1365-313X.2010.04213.x (2010).

40 Raschke, K. Simultaneous requirement of carbon dioxide and abscisic acid for stomatal closing in Xanthium strumarium L. *Planta* **125**, 243-259, doi:10.1007/BF00385601 (1975).

41 Webb, A. A. & Hetherington, A. M. Convergence of the abscisic acid, CO_2, and extracellular calcium signal transduction pathways in stomatal guard cells. *Plant Physiol* **114**, 1557-1560 (1997).

42 Nishimura, N. *et al.* PYR/PYL/RCAR family members are major in-vivo ABI1 protein phosphatase 2C-interacting proteins in Arabidopsis. *Plant J* **61**, 290-299, doi:10.1111/j.1365-313X.2009.04054.x (2010).

43 Yin, Y. *et al.* Difference in abscisic acid perception mechanisms between closure induction and opening inhibition of stomata. *Plant Physiol* **163**, 600-610, doi:10.1104/pp.113.223826 (2013).

44 Hsu, P. K. *et al.* Abscisic acid-independent stomatal CO2 signal transduction pathway and convergence of CO2 and ABA signaling downstream of OST1 kinase. *Proc Natl Acad Sci U S A* **115**, E9971-E9980, doi:10.1073/pnas.1809204115 (2018).

45 Bensmihen, S. *et al.* Analysis of an activated ABI5 allele using a new selection method for transgenic Arabidopsis seeds. *FEBS Lett* **561**, 127-131, doi:10.1016/S0014-5793(04)00148-6 (2004).

46 Deblaere, R. *et al.* Efficient octopine Ti plasmid-derived vectors for Agrobacterium-mediated gene transfer to plants. *Nucleic Acids Res* **13**, 4777-4788 (1985).

47 Clough, S. J. & Bent, A. F. Floral dip: a simplified method for Agrobacterium-mediated transformation of Arabidopsis thaliana. *Plant J* **16**, 735-743 (1998).

48 Huang, S. *et al.* Ca^{2+} signals in guard cells enhance the efficiency by which ABA triggers stomatal closure. *New Phytol*, doi:10.1111/nph.15985 (2019).

49 Geiger, D. *et al.* Stomatal closure by fast abscisic acid signaling is mediated by the guard cell anion channel SLAH3 and the receptor RCAR1. *Sci Signal* **4**, ra32, doi:10.1126/scisignal.2001346 (2011).

50 Geilfus, C. M., Tenhaken, R. & Carpentier, S. C. Transient alkalinization of the leaf apoplast stiffens the cell wall during onset of chloride salinity in corn leaves. *J Biol Chem* **292**, 18800-18813, doi:10.1074/jbc.M117.799866 (2017).

51 Huber, W. *et al.* Orchestrating high-throughput genomic analysis with Bioconductor. *Nat Methods* **12**, 115-121, doi:10.1038/nmeth.3252 (2015).

52 R_Development_Core_Team. R: A Language and Environment for Statistical Computing. *Vienna, Austria, R Foundation for Statistical Computing* (2011).

53 Shi, W., Oshlack, A. & Smyth, G. K. Optimizing the noise versus bias trade-off for Illumina whole genome expression BeadChips. *Nucleic Acids Res* **38**, e204, doi:10.1093/nar/gkq871 (2010).

54 Ritchie, M. E. *et al.* limma powers differential expression analyses for RNA-sequencing and microarray studies. *Nucleic Acids Res* **43**, e47, doi:10.1093/nar/gkv007 (2015).

55 Benjamini, Y. & Hochberg, Y. Controlling the false discovery rate - a practical and powerful approach to multiple testing. *J Roy Stat Soc B Met* **57**, 289-300 (1995).

56 Wu, D. & Smyth, G. K. Camera: a competitive gene set test accounting for inter-gene correlation. *Nucleic Acids Research* **40**, e133, doi:10.1093/nar/gks461 (2012).

57 Gentleman, R. C. *et al.* Bioconductor: open software development for computational biology and bioinformatics. *Genome Biol* **5**, R80, doi:10.1186/gb-2004-5-10-r80 (2004).

58 Szklarczyk, D. *et al.* The STRING database in 2011: functional interaction networks of proteins, globally integrated and scored. *Nucleic acids research* **39**, D561-568, doi:10.1093/nar/gkq973 (2011).

59 Dittrich, M. T., Klau, G. W., Rosenwald, A., Dandekar, T. & Muller, T. Identifying functional modules in protein-protein interaction networks: an integrated exact approach. *Bioinformatics* **24**, i223-231, doi:10.1093/bioinformatics/btn161 (2008).

60 Beisser, D., Klau, G. W., Dandekar, T., Muller, T. & Dittrich, M. T. BioNet: an R-Package for the functional analysis of biological networks. *Bioinformatics* **26**, 1129-1130, doi:10.1093/bioinformatics/btq089 (2010).

61 Zeileis, A. Econometric Computing with HC and HAC Covariance Matrix Estimators. *Journal of Statistical Software* **11**, 1-17, doi:10.18637/jss.v011.i10 (2004).

62 Hothorn, T., Bretz, F. & Westfall, P. Simultaneous inference in general parametric models. *Biom J* **50**, 346-363, doi:10.1002/bimj.200810425 (2008).

Figure legends

Fig. 1 Guard cell signalling pathway analysis. MapMan pathways with a significant enrichment in at least one stimulus are visualized in a heatmap. Pathways are listed in rows and stimuli in columns. Darker shades (corresponding to the negative decadic logarithm of the enrichment pvalue) depict more significant enrichments. For each treatment and the respective controls four microarrays were analysed except darkness (n=3). All replicates represent biologically independent samples. A competitive pathway enrichment test was performed as implemented in the camera function from the limma package based on the gene expression data.

Fig. 2 Integrative networks analysis identify distinct stomatal closing signal modules. Stimulus specific modules: Optimal responsive sub networks of regulated genes in the entire network for a, ABA, b, RH, c, darkness, and d, CO_2 stimulation. Circles denote positive scoring genes (with highly significant expression changes)

911 whereas rectangles denote negative scoring nodes (e.g. additional nodes of modest
912 regulation) which are implicated by the algorithm on the bases of their functional
913 network context. Red indicates up regulation, green down regulation, where darker
914 colours correspond to higher fold change values. Gene clusters of common cellular
915 processes are enclosed by shaded lines highlighting the functional sub structure of
916 the modules. Only ABA-responsive genes are named (for details see Supplementary
917 Fig. 2). e, ABA receptors are main components in adaptation to stomatal closing
918 signals. Each module contains a cluster of typical ABA responsive genes. In all cases
919 ABA receptors are affected. Among the closing signals the kind of receptors as well
920 as the direction of regulation differ markedly indicating an altered sensitivity towards
921 ABA in the adaptation process to the individual signals. For each treatment and the
922 respective controls four microarrays were analysed except darkness (n=3). All
923 replicates represent biologically independent samples. The network analysis is based
924 on the statistics and p-values described in Table S1a.
925
926 **Fig. 3. PYL2 is sufficient for stomatal ABA sensitivity.** Excised leaves, in
927 darkness were preincubated with ABA fed via the petiole to prevent stomatal opening
928 in the light. Stomatal aperture was measured by gas exchange as a function of
929 relative transpiration. a, Stomata of wildtype and the 11458-mutant (PYL2 present)
930 remained almost closed, while those of the 12458-mutant appeared ABA-insensitive.
931 b, PYL2 in the 12458-background fully restored the wildtype phenotype, while PYR1
932 reacted with incomplete ABA-sensitivity. c, PYL4 and PYL5 were unable to restore
933 ABA sensitivity of the 12458-quintuple background line. Values are normalized to
934 timepoint 0. n=28 for Col0, n=6 for 12458, n=9 for 11458, n=5 for PYR1::12458, n=5

for PYL2::12458, n=6 for PYL4::12458, n=7 for PYL5::12458. All replicate numbers represent biologically independent samples, mean±SE.

Fig. 4. ABA-induced movements of individual stoma. Electro-infusion of ABA to single stoma. a, Stomata of wildtype, 11458-mutants (PYL2 present) and the PYL2::12458 complementation line closed within 10 minutes following an ABA-pulse. In contrast, stomata of the 12458-mutant (without PYL2) and the PYL5::12458 complementation line remained fully open. b, Amplitudes of the changes in stomatal pore width from fully open to maximum closed after ABA infusion revealed that PYL2 presence is sufficient to close stomata to wildtype levels. Stomata of the 12458 mutant remained open. In contrast to all other samples, the width of PYL5::12458 stomata showed little but ABA-independent closure over time. c, stomatal width of wildtype and mutants after 20 minutes illumination. Only 12458 mutants showed significantly wider stomatal pores prior to ABA application. n=9, all replicate numbers represent biologically independent samples, mean±SE.

Fig. 5 PYL4 and 5 render guard cells CO_2-sensitive. Whole plants were placed in gas exchange cuvettes in the dark at 400 ppm CO2 and stomatal aperture was measured as a function of the relative transpiration by gas exchange. Following stomatal opening in the light the CO_2 concentration was increased to 1000 ppm. a, Stomata of wildtype plants closed about 60%, while both quintuple-mutants did not react. b, The PYL2 complemented 12458-mutant did not react to elevated CO_2 and also the PYR1 complemented stomata remained impaired. c, 12458-mutants complemented with either PYL4 or PYL5 closed their stomata in a wildtype manner. Values are normalized to timepoint 0. n=20 for Col0, n=12 for 12458, n=6 for 11458,

960 n=4 for PYR1::12458, n=6 for PYL2::12458 and n=7 for PYL5::12458. All replicate
961 numbers represent biologically independent samples, mean ± SE.
962

PYR1	At4g17870					64
PYL1	At5g46790					
PYL2	At2g26040				39	18
PYL4	At2g38310			66	36	19
PYL5	At5g05440				33	16
PYL8	At5g53160				77	54
MYB60	At1g08810					42
ABR	At3g02480				1331	5679
HAI1	At5g59220		173*		594	1535
ABA		25 nM	100 nM	250 nM	2,5 µM	25 µM

963

964 **Table 1 ABA-dose-response of the transcription of guard cell ABA-receptor**
965 **and ABA-regulated genes.** Upon ABA-spray application transcription was either
966 induced, reduced or remained unchanged. Numbers represent the expression
967 changes presented in Supplementary Fig.3 (in percent) relative to untreated control.
968 Blue = down-regulation, yellow to red = up-regulation, grey = no change in
969 expression. Asterisk denotes that this value has weak significance and represents
970 only 11 % of the maximum induction (for sample sizes and statistics see related
971 Supplementary Fig. 3 and Methods).
972

	MYB60	ABI2	CIPK25	KCR2	RAB18
wt	26	268	268	195	400
12458 (PYL1 present)		298	269	285	1218
PYR1::12458	40		303	194	1436
PYL2::12458	38	251	228	200	731
PYL4::12458		307	331	244	491
PYL5::12458		314			381
11458 (PYL2 present)	31				649

PYR1::11458	22	203			956
PYL1::11458	14	160	178		433
PYL4::11458	25				421
PYL5::11458	25				301
PYL8::11458	43		215		493

Table 2 Individual ABA receptor family members control the expression of downstream genes. ABA-spraying (25 µM) led to up or downregulation of genes in wildtype plants. Quintuple knockout and complementation lines revealed the receptors necessary for ABA-induced gene-regulation. Numbers represent the expression changes presented in Supplementary Fig.6 (in percent) relative to untreated control. Blue = downregulation, yellow to red = up-regulation, grey = no change in expression. (for sample sizes and statistics see related Supplementary Fig. 6 and Methods).

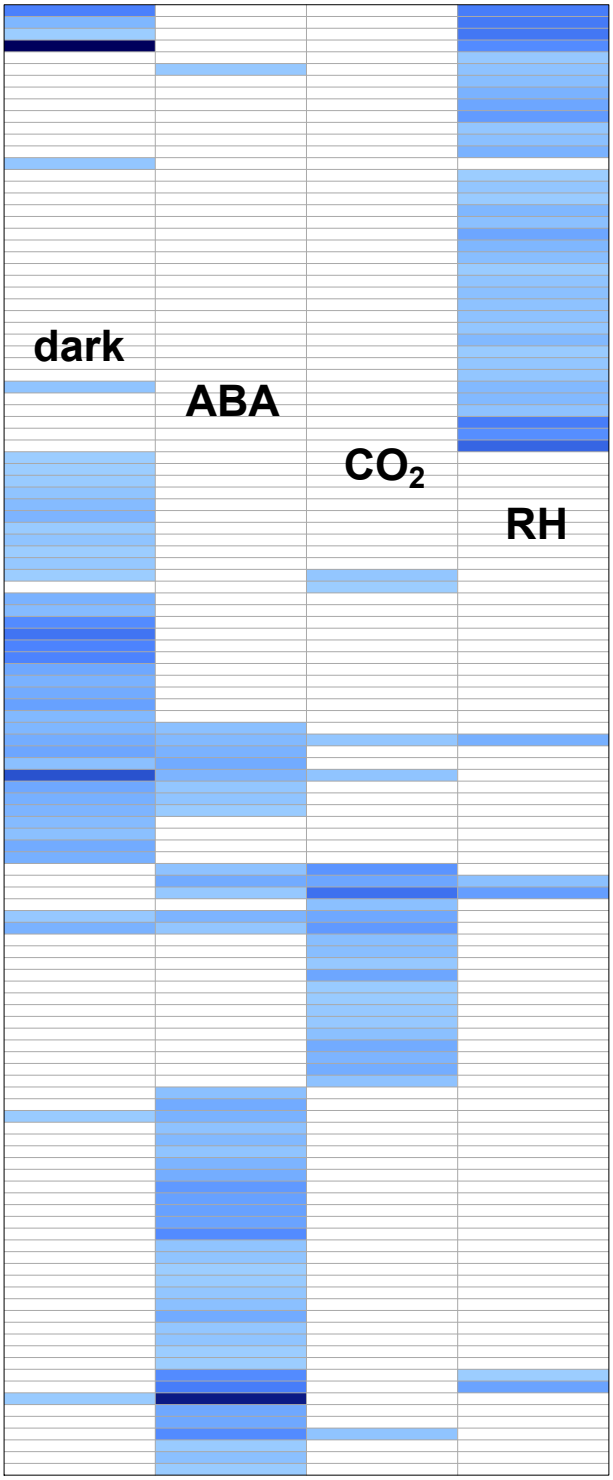
dark
ABA
CO_2
RH

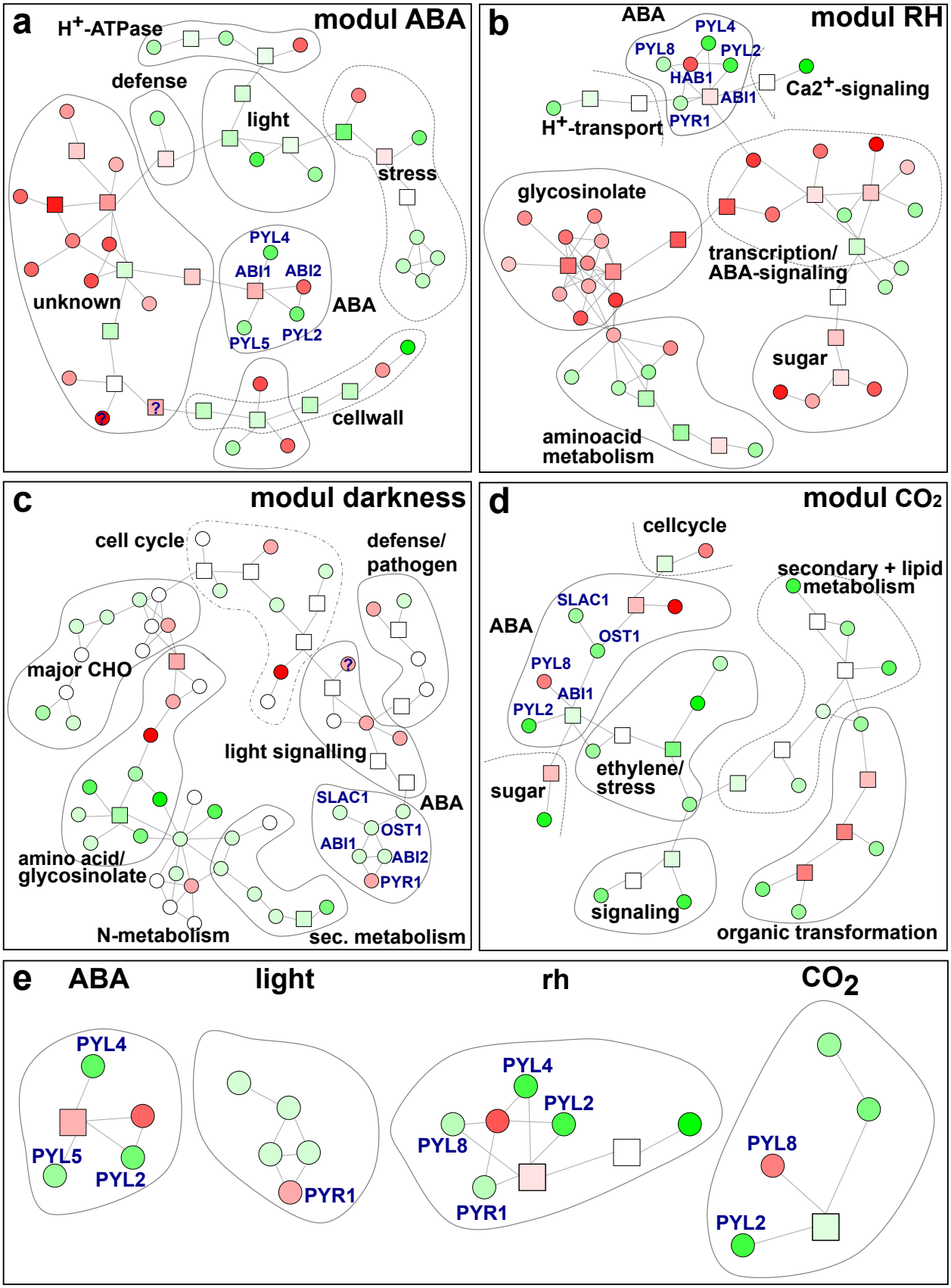
a
modul ABA
H+-ATPase
defense
light
stress
unknown
PYL4
ABI1
ABI2
ABA
PYL5
PYL2
cellwall
b
modul RH
ABA
PYL4
PYL8
PYL2
HAB1
ABI1
Ca2+-signaling
H+-transport
PYR1
glycosinolate
transcription/
ABA-signaling
sugar
aminoacid
metabolism
c
modul darkness
cell cycle
defense/
pathogen
major CHO
light signalling
SLAC1
ABA
OST1
ABI1
ABI2
PYR1
amino acid/
glycosinolate
N-metabolism
sec. metabolism
d
modul CO2
cellcycle
secondary + lipid
metabolism
SLAC1
ABA
OST1
PYL8
ABI1
PYL2
sugar
ethylene/
stress
signaling
organic transformation
e
ABA
light
rh
CO2
PYL4
PYL5
PYL2
PYR1
PYL4
PYL2
PYL8
PYR1
PYL8
PYL2

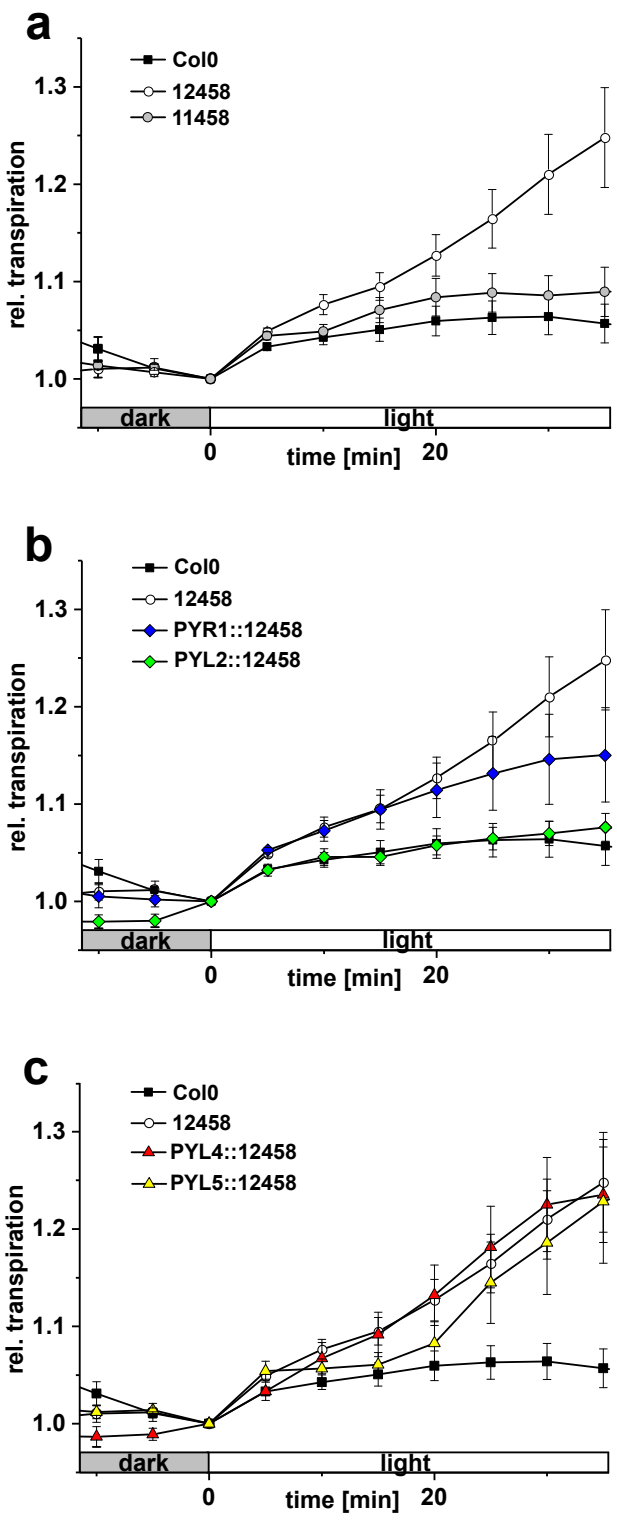
a
Col0
12458
11458
rel. transpiration
1.3
1.2
1.1
1.0
dark
light
0
time [min]
20
b
Col0
12458
PYR1::12458
PYL2::12458
rel. transpiration
1.3
1.2
1.1
1.0
dark
light
0
time [min]
20
c
Col0
12458
PYL4::12458
PYL5::12458
rel. transpiration
1.3
1.2
1.1
1.0
dark
light
0
time [min]
20

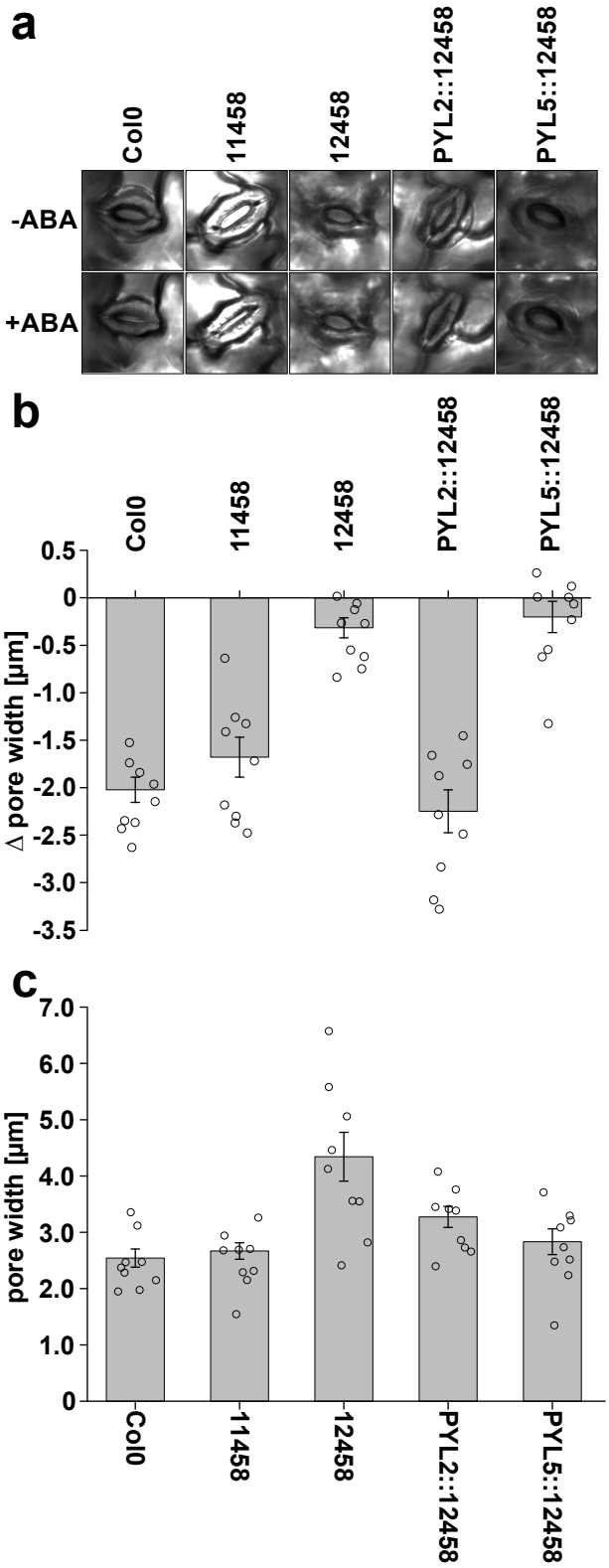
a
Col0
11458
12458
PYL2::12458
PYL5::12458
-ABA
+ABA
b
Col0
11458
12458
PYL2::12458
PYL5::12458
Δ pore width [µm]
0.5
0
-0.5
-1.0
-1.5
-2.0
-2.5
-3.0
-3.5
c
pore width [µm]
7.0
6.0
5.0
4.0
3.0
2.0
1.0
0
Col0
11458
12458
PYL2::12458
PYL5::12458

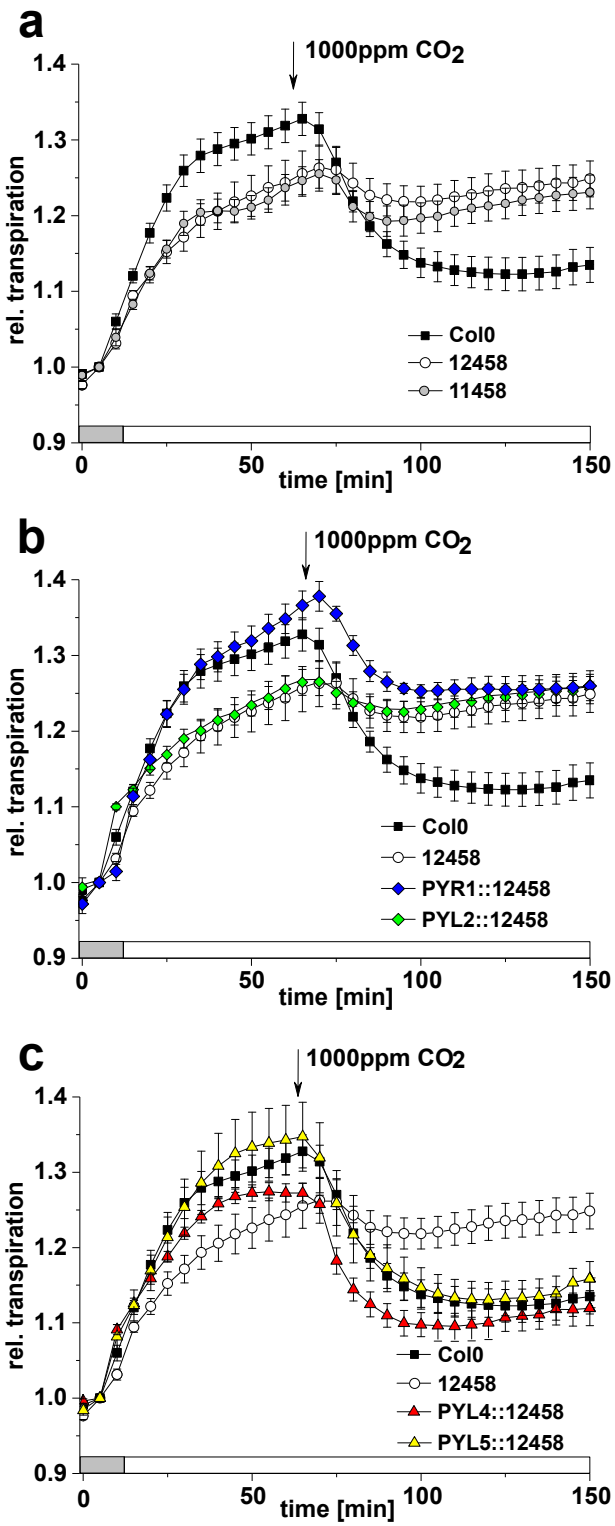
a
1000ppm CO2
rel. transpiration
time [min]
Col0
12458
11458
b
1000ppm CO2
rel. transpiration
time [min]
Col0
12458
PYR1::12458
PYL2::12458
c
1000ppm CO2
rel. transpiration
time [min]
Col0
12458
PYL4::12458
PYL5::12458